Water Resources Research

RESEARCH ARTICLE
10.1029/2020WR027529

An Analytical Solution of Groundwater Flow in a Confined Aquifer With a Single-Well Circulation System

Kun Tu[1,2,3], Qiang Wu[1,2], Jirka Simunek[3], Chaofan Chen[4,5], Ke Zhu[1,2], Yifan Zeng[1,2], Shengheng Xu[1,2], and Yang Wang[6]

[1]College of Geoscience and Surveying Engineering, China University of Mining and Technology, Beijing, China, [2]National Engineering Research Center of Coal Mine Water Hazard Controlling, Beijing, China, [3]Department of Environmental Sciences, University of California, Riverside, CA, USA, [4]Helmholtz Centre for Environmental Research (UFZ), Leipzig, Germany, [5]Applied Environmental Systems Analysis, Dresden University of Technology, Dresden, Germany, [6]Central Plains Institute of Intelligent Geology, Zhengzhou, China

Key Points:
- A general mathematical model describing groundwater flow in a confined aquifer for a single-well circulation system is developed
- An analytical solution for drawdown in the Laplace domain and the steady-state analytical solution in the time domain are obtained
- The characteristics of groundwater flow and the effects of different parameters on drawdown are investigated

Correspondence to:
Q. Wu,
wuq@cumtb.edu.cn

Citation:
Tu, K., Wu, Q., Simunek, J., Chen, C., Zhu, K., Zeng, Y., et al. (2020). An analytical solution of groundwater flow in a confined aquifer with a single-well circulation system. *Water Resources Research*, *56*, e2020WR027529. https://doi.org/10.1029/2020WR027529

Received 20 MAR 2020
Accepted 9 JUN 2020
Accepted article online 12 JUN 2020

Abstract In this study, a general analytical model for the single-well circulation system is developed to analyze transient drawdown in a confined aquifer. The analytical solution of transient drawdown in the Laplace domain, which is numerically inverted into the time domain using the Stehfest method, is derived by employing a combination of the Laplace and Fourier cosine transforms. The characteristics of transient drawdown and the effects of different parameters related to the single-well circulation system on drawdown are investigated. Furthermore, the analytical solution under steady-state conditions is obtained using the Fourier cosine transform. The results show that steady drawdown contours are symmetric around a horizontal midplane of an aquifer and vary tremendously with distance from the well axis. The contours of drawdown around the sealed section are dense, meaning that the hydraulic gradient in this area is relatively large. The sensitivity analysis, performed to evaluate the characteristics of drawdown to changes in each parameter, indicates that the radial hydraulic conductivity and the length of the sealed section have a large impact on the drawdown and that each parameter has its influence period on the drawdown.

1. Introduction

Among different types of groundwater heat pump systems, the single-well circulation groundwater heat pump system is different from conventional groundwater heat pump systems—for example, a well doublet system (Banks, 2009; Galgaro & Cultrera, 2013) or a standing column well system (Abu-Nada et al., 2008; Deng et al., 2005—especially in terms of the well structure. In a single-well circulation system (Figure 1), a single borehole is divided into two sections by well packers (the gray section in Figures 1 and 2), which are placed in the middle of a single borehole to block injected water in the injection section of the well from flowing to the pumping section of the well. The single-well circulation systems can be regarded as a combination of two partially penetrating wells. The lower one is a pumping well, from which groundwater is pumped at a rate Q, and the upper one is an injection well for injecting water at the same rate Q.

A single-well circulation groundwater heat pump system is a new technology that emerged in 2001 and since then has been employed to provide heating and cooling for buildings in China (Xu & Rybach, 2003). This unique groundwater heat pump system has gained tremendous interest and has been increasingly used during the last two decades, especially in northern China. Although the system has many practical applications, the theoretical investigation of this system is somewhat limited. Xu and Rybach (2005) presented the development and several successful engineering implementations of this original and innovative technology in terms of system designs, energy savings, and environmental protection. Wu et al. (2015) compared the single-well circulation system with other conventional groundwater heat pump systems in terms of the well configuration, requirements on hydrogeological and thermal geological conditions, environmental impacts, regulatory requirements, and so forth. Rybach (2015) presented engineering applications in China and other countries and summarized operational principles of the single-well circulation groundwater heat pump

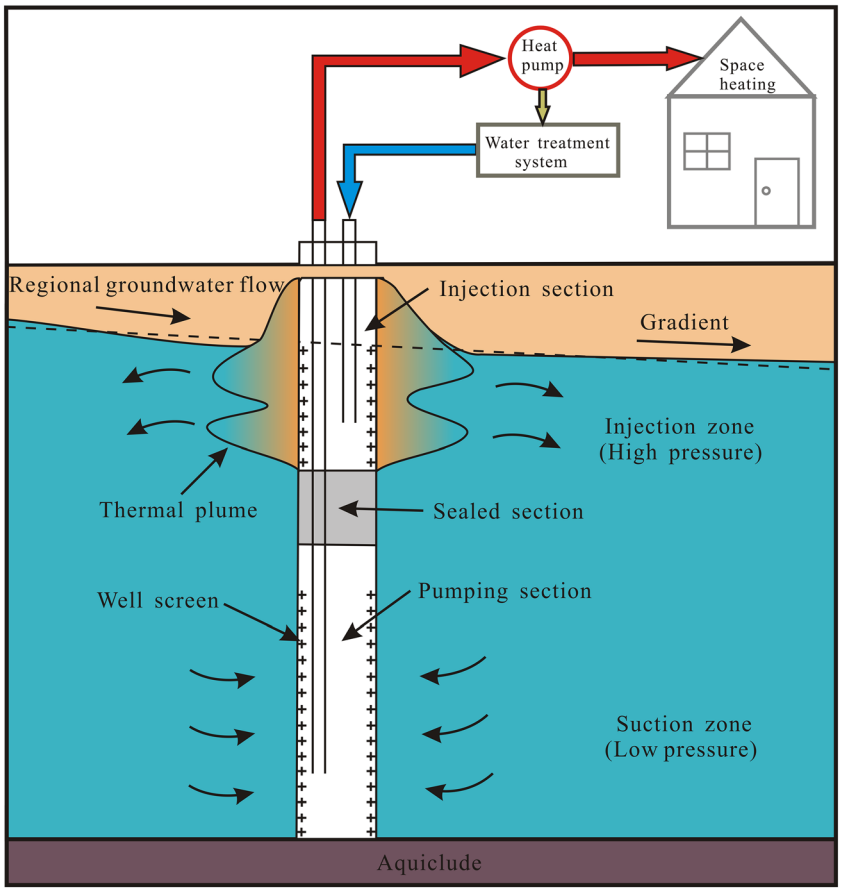

Figure 1. An overview of a single-well circulation system for shallow geothermal energy extraction (Wu et al., 2019).

system. Finally, Zeng et al. (2017) provided a detailed discussion on energy efficiency, cost-effectiveness, operation, and maintenance of this system using a case study in Nebraska.

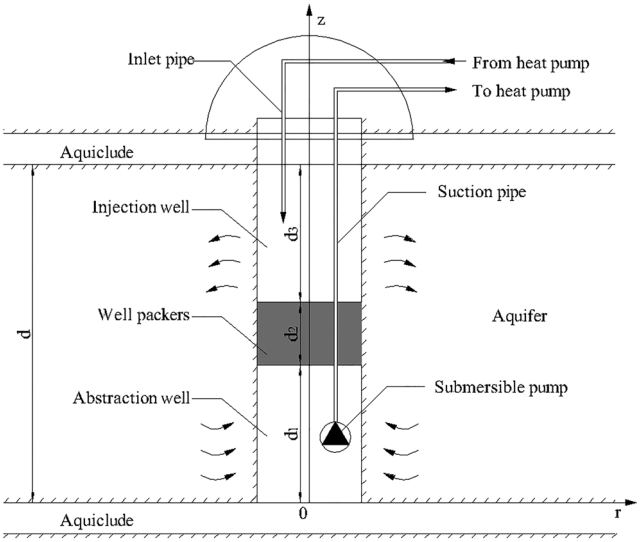

Figure 2. The schematic diagram of a single-well circulation system.

The heat exchange in a single-well circulation groundwater heat pump system is a result of combined groundwater flow and heat transport. Heat convection, in particular, is influenced by fluid flow. Therefore, a good understanding of groundwater flow is an especially vital and essential step before one can start studying the heat exchange in a single-well circulation groundwater heat pump system. Up to now, most of the research on groundwater flow focused on fully or partially penetrating wells.

The topic of drawdown around a fully penetrating well has been discussed in many works. For instance, Theis (1935) was the first who presented an analytical solution describing groundwater flow toward a fully penetrating well in a confined aquifer of an infinite extent. Later, Papadopulos and Cooper (1967) proposed a mathematical model describing groundwater flow in a confined aquifer while considering the influence of the well radius and wellbore storage. Chen (1984) derived, based on several existing solutions, an analytical solution describing groundwater flow in a finite confined aquifer with a zero drawdown condition at the exterior boundary. Novakowski (1989) obtained a Laplace domain solution of drawdown in a composite confined aquifer while considering the effects of the well radius and wellbore storage. Subsequently, Yeh et al. (2003) presented an analytical solution describing the head distribution for a slug test in a two-zone confined aquifer system. Wen and Zhan (2008)

Table 1
Comparison of Analytical Models for Partially and Fully Penetrating Wells

Model	Well structure	Well radius	Groundwater flow	Skin effect	Type of aquifer
This study	Two partially penetrating wells in one wellbore	Zero	Darcian flow	No	A confined aquifer with an infinite areal extent
Theis (1935)	A fully penetrating well	Zero	Darcian flow	No	A confined aquifer with an infinite areal extent
Chen (1984)	A fully penetrating well	Zero	Darcian flow	No	A finite confined aquifer
Wen and Zhan (2008)	A fully penetrating well	Zero/Finite	non-Darcian flow	No	A confined aquifer with an infinite areal extent
Lin et al. (2016)	A fully penetrating well	Finite	Darcian flow	Yes	A two-zone confined aquifer with a finite areal extent
Hantush (1961)	A partially penetrating well	Zero	Darcian flow	No	A confined aquifer with an infinite areal extent
Chiu et al. (2007)	A partially penetrating well	Finite	Darcian flow	Yes	A two-zone confined aquifer with an infinite areal extent
Wen et al. (2013)	A partially penetrating well	Zero	non-Darcian flow	No	A confined aquifer with an infinite areal extent
Feng and Wen (2016)	A partially penetrating well	Finite	non-Darcian flow	Yes	A two-zone confined aquifer with an infinite areal extent

proposed a general analytical model describing non-Darcian groundwater flow in a confined aquifer by employing a combination of the power law function and a linearization procedure. Wang et al. (2012) presented an analytical solution describing groundwater flow while considering a constant-flux pumping along a finite radius well in the skin zone. Lin et al. (2016) proposed an analytical model describing groundwater flow in a composite confined aquifer of a finite extent induced by a pumping test while considering the effect of the well skin and a Robin-type outer boundary.

There are also a lot of studies available in the literature regarding groundwater flow to a partially penetrating well (Table 1). The first mathematical model for a partially penetrating well was presented by Hantush (1957), who derived an analytical solution by applying the Laplace and Fourier cosine transforms. Since then, partially penetrating well systems have been investigated by many other researchers (e.g., Ataie-Ashtiani et al., 2012; Chang & Chen, 2002; Chang & Yeh, 2009; Chen et al., 2010; Chiu et al., 2007; Yang & Yeh, 2005; Zlotnik et al., 1998). For instance, steady-state flow in an unconfined aquifer to one or multiple partially penetrating wells was studied by Luther and Haitjema (1999). Yang and Yeh (2005) presented a semianalytical solution describing groundwater flow toward a partially penetrating well induced by the constant head test in an infinite extent aquifer. Taking into account the effect of a finite-thickness skin, Chiu et al. (2007) presented an analytical solution for a drawdown of groundwater flow to a partially penetrating well. Barua and Bora (2010) presented a steady-state solution for groundwater flow induced by pumping in a partially penetrating well in a finite confined aquifer associated with the condition of the constant head at the outer boundary. Ataie-Ashtiani et al. (2012) derived an analytical solution for the capture zone of a partially penetrating well with an infinitesimally small well radius and a fixed pumping rate Q. By employing the Izbash equation and a linearization procedure, Wen et al. (2013) presented an approximate analytical solution, which can describe the non-Darcian flow toward a partially penetrating well in a confined aquifer. Feng and Wen (2016) proposed an analytical model describing non-Darcian flow toward a partially penetrating well in a confined aquifer, which considered the effects of the well skin. Table 1 summarizes and compares the available, above-mentioned analytical models.

However, compared with the studies mentioned above of groundwater flow in an aquifer with fully or partially penetrating wells, the research on a particular well structure of a single-well circulation system is quite limited. Only a few studies (Ni et al., 2011; Sorensen & Reffstrup, 1992; Tu et al., 2019) dealing with groundwater flow in an aquifer with a single-well circulation system can be found in the literature. Sorensen and Reffstrup (1992) were the first to present a simplified mathematical model for the analysis of groundwater flow and heat transport for a new type of a groundwater heat pump system, which can extract and inject groundwater with one well borehole. Ni et al. (2011) developed a mathematical model describing groundwater flow induced by a single-well system in a leaky confined aquifer. Based on the superposition principle and by adopting the analytical solution of a partially penetrating well derived by Hantush (1961), Ni et al. (2011) obtained their solution by summing up the analytical solutions for these two partially penetrating wells. Although it is convenient to obtain analytical solutions using the superposition principle, this approach inevitably introduces problems such as complicated well configuration functions. The Hantush

and Jacob well function (Hantush, 1961) makes the analytical solution more complicated and increases its instability and computational cost. Subsequently, Tu et al. (2019) derived a closed-form, steady-state analytical solution to investigate groundwater flow in a confined aquifer by employing the separation variable method and the Laplace transform. However, their solution still includes the complicated Hantush and Jacob well function and the well configuration function. Therefore, to overcome the above-mentioned problems, we aim at rigorously deriving the analytical solution based on the governing equation for a single-well circulation system by employing a combination of the Laplace and Fourier cosine transforms.

The main objective of this work is to develop a general analytical mathematical model describing groundwater flow in a confined aquifer for a single-well circulation system with a unique well structure with two partially penetrating wells in one single wellbore. The analytical solution for drawdown in the Laplace domain is obtained by employing the Laplace and Fourier cosine transforms. The effects of the hydraulic conductivity, the length of the sealed section, and other parameters on the drawdown distribution were analyzed, which to our knowledge have not been investigated by other researchers. The steady-state solution in the time domain is also derived. The analytical solution of transient drawdown is used in the sensitivity analysis to investigate the effects of different parameters on drawdown and to identify which of these parameters must be carefully considered when designing a single-well circulation system.

2. Mathematical Model

In order to investigate groundwater flow in a single-well circulation system, a mathematical model was developed, as shown in Figure 2. The assumptions of this mathematical model are as follows: (1) A confined aquifer is assumed to be homogeneous, anisotropic, and infinite in the horizontal direction; (2) underlying and overlying rocks are considered to be impermeable, homogeneous, anisotropic, and of uniform thickness; (3) groundwater flow in a confined aquifer follows Darcy's law; (4) the storage and release of groundwater due to rising and decreasing hydraulic heads are instantaneous; (5) pumping and injection rates Q (positive for pumping and negative for injection) are constant; and (6) the well radius is infinitesimally small and can be regarded as 0.

2.1. Governing Equation

Base on the above-listed assumptions, the equation describing groundwater flow in a confined aquifer can be written as follows:

$$K_r\left(\frac{\partial^2 s(r,\,z,\,t)}{\partial r^2}+\frac{1}{r}\frac{\partial s(r,\,z,\,t)}{\partial r}\right)+K_z\frac{\partial^2 s(r,\,z,\,t)}{\partial z^2}=S\frac{\partial s(r,\,z,\,t)}{\partial t}, \tag{1}$$

where r is the radial coordinate (L); t denotes time (T); s is groundwater drawdown (L); K_r and K_z represent the horizontal and vertical hydraulic conductivities, respectively (LT^{-1}); and S refers to the specific storage of an aquifer (L^{-1}).

2.2. Initial Conditions

Initial drawdown in a confined aquifer at time $t = 0$ is assumed to be constant and equal to 0:

$$s(r,\,z,\,0)=0. \tag{2}$$

2.3. Boundary Conditions

The boundary conditions in infinity in the radial direction and at the top and bottom of a confined aquifer, $r = \infty$, $z = d$, and $z = 0$, respectively, are given as follows:

$$s(\infty,\,z,\,t)=0 \tag{3}$$

and

$$\frac{\partial s(r,\,d,\,t)}{\partial z}=0 \tag{4}$$

and

$$\frac{\partial s(r,\,0,\,t)}{\partial z}=0, \tag{5}$$

where z is the vertical coordinate (L) and d denotes the thickness of a confined aquifer (L). The boundary conditions at the rim of the wellbore are as follows:

$$\lim_{r\to 0} r\frac{\partial s}{\partial r}=\begin{cases}\dfrac{-Q}{2\pi K_r d_1} & (0\le z\le d_1)\\ 0 & (d_1\le z\le d_1+d_2)\\ \dfrac{Q}{2\pi K_r d_3} & (d_1+d_2\le z\le d)\end{cases}, \tag{6}$$

where d_1, d_2, and d_3 are the lengths of pumping, sealed, and injection sections, respectively (L), and Q represents pumping and injection rates (L^3T^{-1}), which are the same and constant in time.

2.4. A General (Transient) Analytical Solution

The mathematical model of a single-well circulation system is fully described using the governing partial differential equation (Equation 1), initial conditions (Equation 2), and boundary conditions (Equations 3–6). This system of equations can be solved by applying the Laplace and Fourier cosine transforms, which convert partial differential equations to ordinary differential equations. A detailed derivation of the analytical solution is given in Appendix A. The analytical solution of drawdown in the Laplace domain is expressed as

$$\bar{s}(r,\,z,\,p)=\sum_{N=1}^{\infty}\frac{Q}{NpK_r\pi^2}\left[\frac{\sin\left(\dfrac{N\pi d_1}{d}\right)}{d_1}+\frac{\sin\left(\dfrac{N\pi(d_1+d_2)}{d}\right)}{d_3}\right]K_0\left(\sqrt{\delta}r\right)\cos\left(\frac{N\pi z}{d}\right), \tag{7}$$

in which $\delta=\dfrac{K_z N^2\pi^2}{K_r\ d^2}+\dfrac{Sp}{K_r}$, $K_0(\cdot)$ denotes zeroth-order modified Bessel functions of the second kind, and p and N (N = 1, 2, 3,...) are the Laplace and Fourier transform variables, respectively.

It is currently not possible to obtain the analytical solution of Equation 7 in the real-time domain due to the Bessel function. However, Equation 7 can be numerically inverted to the real-time domain using several numerical inversion methods (e.g., Crump, 1976; De Hoog et al., 1982; Stehfest, 1970a, 1970b). In this study, the Stehfest method is utilized to invert the Laplace domain solution numerically and to calculate drawdown in the real-time domain. The detailed introduction of the Stehfest method can be found in Stehfest (1970a, 1970b).

A MATLAB program has been developed to calculate drawdown in the Laplace domain, which is then inverted numerically using the Stehfest method. This inversion method requires as input the number of terms used in the inversion, n, and the number of terms of the infinite series, N. Numerical tests indicate that the choice of $n = 20$ and $N \ge 10$ gives accurate and stable results. To reduce the computational cost, $n = 20$ and $N = 10$ are used in all calculations.

2.5. A Steady-State Analytical Solution

When the pumping and injection times are large, namely, $t \to \infty$, the groundwater flow will reach a quasi-steady state. In this case, drawdown around partially penetrating wells stops changing with time. Therefore, we have

$$\frac{\partial s(r,\,z,\,t)}{\partial t}=0. \tag{8}$$

Then, Equation 1 can be reduced to

$$K_r\left(\frac{\partial^2 s(r,\,z)}{\partial r^2}+\frac{1}{r}\frac{\partial s(r,\,z)}{\partial r}\right)+K_z\frac{\partial^2 s(r,\,z)}{\partial z^2}=0. \tag{9}$$

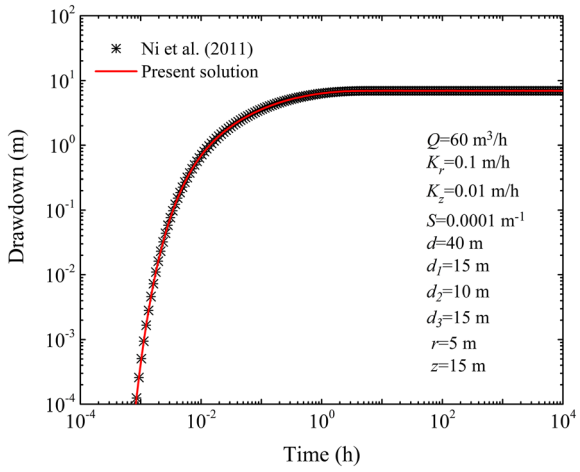

Figure 3. Comparison of the newly derived analytical solution for drawdown (Equation 7) with the result of Ni et al. (2011) for parameters given in the figure.

Applying the Fourier cosine transform to the second-order partial derivative with respect to the z coordinate, the partial differential equation 9 is solved (see Appendix B) to give

$$s(r,z)=\sum_{N=1}^{\infty}\frac{Q}{NK_r\pi^2}\left[\frac{\sin\left(\frac{N\pi d_1}{d}\right)}{d_1}+\frac{\sin\left(\frac{N\pi(d_1+d_2)}{d}\right)}{d_3}\right]K_0\left(\sqrt{\delta'}r\right)\cos\left(\frac{N\pi z}{d}\right), \tag{10}$$

where $\delta'=\frac{K_z}{K_r}\left(\frac{N\pi}{d}\right)^2$.

According to Darcy's Law, steady-state groundwater fluxes can be obtained from the analytical solution for steady-state drawdown (Equation 10) as follows:

$$\begin{cases} v_r=K_r\dfrac{\partial s}{\partial r} \\ v_z=K_z\dfrac{\partial s}{\partial z} \end{cases}. \tag{11}$$

According to the properties of the modified Bessel function, the mathematical relation $\frac{dK_0(x)}{dx}=-K_1(x)$, where x is the variable of the modified Bessel function. Thus, Equation 11 can be written as

$$\begin{cases} v_r=\sum_{N=1}^{\infty}\dfrac{-Q}{\pi d}\sqrt{\dfrac{K_z}{K_r}}\left[\dfrac{\sin\left(\frac{N\pi d_1}{d}\right)}{d_1}+\dfrac{\sin\left(\frac{N\pi(d_1+d_2)}{d}\right)}{d_3}\right]K_1\left(\sqrt{\delta'}r\right)\cos\left(\dfrac{N\pi z}{d}\right) \\ v_z=\sum_{N=1}^{\infty}\dfrac{-QK_z}{\pi dK_r}\left[\dfrac{\sin\left(\frac{N\pi d_1}{d}\right)}{d_1}+\dfrac{\sin\left(\frac{N\pi(d_1+d_2)}{d}\right)}{d_3}\right]K_0\left(\sqrt{\delta'}r\right)\sin\left(\dfrac{N\pi z}{d}\right) \end{cases}. \tag{12}$$

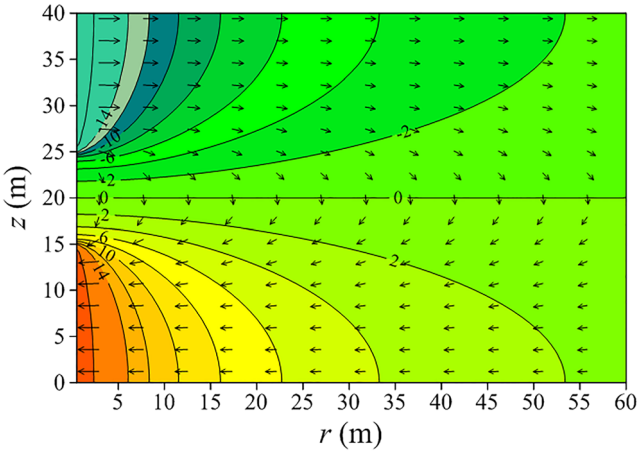

Figure 4. Contours of steady-state drawdown and steady-state flux vectors in a single-well circulation system.

3. Results and Discussion

3.1. Verification of the Analytical Solution

First, the newly derived analytical solution for transient drawdown is verified by comparing its results with the solution of Ni et al. (2011). In their work, a single-well circulation system is regarded as a combination of one partially penetrating well for injection and another one for pumping. The analytical solution for a partially penetrating well was developed by Hantush (1961). Based on the superposition principle, Ni et al. (2011) obtained the analytical solution by summing up the analytical solutions for these two partially penetrating wells in a single-well circulation system. These analytical solutions (i.e., Equation 7 and Ni et al., 2011) for a single-well circulation system are used to calculate transient groundwater drawdown for a system with the following parameters: Q = 60 m^3/hr, K_r = 0.1 m/hr, K_z = 0.01 m/hr, S = 0.0001 m^{-1}, d = 40 m, d_1 = 15 m, d_2 = 10 m, and d_3 = 15 m, at r = 5 m and z = 15 m. Figure 3 shows that the results of the newly derived analytical solution correspond very well with the solution of Ni et al. (2011).

3.2. Steady-State Drawdown

Figure 4 depicts contours for steady-state drawdown and steady-state flux vectors (Equations 10 and 12, respectively) in a single-well circulation

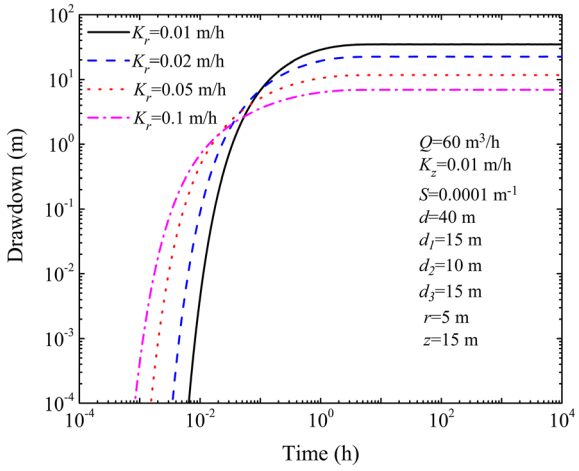

Figure 5. The effect of the radial hydraulic conductivity (K_r) on drawdown with time (for parameters given in the figure).

system. The following parameters (the same as in Figure 3) were used in this scenario: $Q = 60$ m^3/hr, $K_r = 0.1$ m/hr, $K_z = 0.01$ m/hr, $S = 0.0001$ m^{-1}, $d = 40$ m, $d_1 = 15$ m, $d_2 = 10$ m, and $d_3 = 15$ m. It can be clearly observed that contours for steady-state drawdown are symmetric around a horizontal midplane of a confined aquifer and vary tremendously with distance from the well axis. The contours of drawdown around the sealed section are dense, indicating that the hydraulic gradient in this area is relatively large. Additionally, due to flow symmetry, absolute values of drawdown are very small around the midplane of a confined aquifer; drawdown is 0 at locations with $z = 20$ m (the middle of a confined aquifer).

3.3. Radial Hydraulic Conductivity

Figure 5 shows the effects of different values of the radial hydraulic conductivity ($K_r = 0.01$, 0.02, 0.05, and 0.1 m/hr) on drawdown with time. Other parameters remain the same as in previous examples; that is, $Q = 60$ m^3/hr, $K_z = 0.01$ m/hr, $S = 0.0001$ m^{-1}, $d = 40$ m, $d_1 = 15$ m, $d_2 = 10$ m, and $d_3 = 15$ m, at $r = 5$ m and $z = 15$ m. It can be seen that drawdown increases with the radial hydraulic conductivity (K_r) at early times, while it decreases as K_r increases at late times. Larger hydraulic conductivities will cause groundwater to react more quickly to the start of water pumping/injection from/into the aquifer at early times, with the depression cone in the suction zone spreading faster, while groundwater can be replenished in a timely manner. Drawdown is thus larger at early times for larger hydraulic conductivities. In contrast, at late times, an increase in drawdown for larger hydraulic conductivities is not as large as for smaller hydraulic conductivities. Moreover, it is worth noting that drawdown converges toward a steady state more quickly for larger radial hydraulic conductivities, as indicated in Figure 5.

3.4. Sealed Section

Figure 6 shows the impact of the length of the sealed section (d_2) on groundwater drawdown in a single-well circulation system. The sealed section is located in the middle of the confined aquifer and between the pumping and injection sections of the well (see Figure 2). The same parameters as in the previous section are used to obtain results displayed in Figure 6, that is, $Q = 60$ m^3/hr, $K_z = 0.01$ m/hr, $S = 0.0001$ m^{-1}, $d = 40$ m, $d_1 = 15$ m, and $d_3 = 15$ m (i.e., $d_1 = d_3$), at $r = 5$ m and $z = 15$ m. Besides, the following lengths of the sealed section are used: $d_2 = 6$, 8, 10, 12, and 14 m, while d_1 and d_3 were correspondingly adjusted to keep d constant. One can observe in Figure 6a that shorter lengths of the sealed section result in larger drawdown at early times, while the length of the sealed section has only a little effect on drawdown at late times. This is due to the fact that shorter lengths of the sealed section require longer lengths of the pumping and injection sections, which require smaller pumping and injection rates for a unit well length (note that the total pumping and/or injection rates are constant). Thus, shorter lengths of the sealed section produce larger

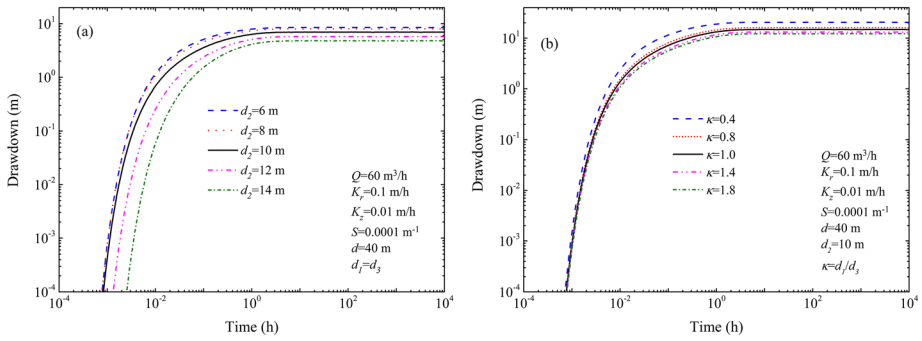

Figure 6. The effect of the length of the sealed section (d_2) when $d_1 = d_3$ (a) and various ratios κ (=d_1/d_3) for a constant d_2 (b) on drawdown with time.

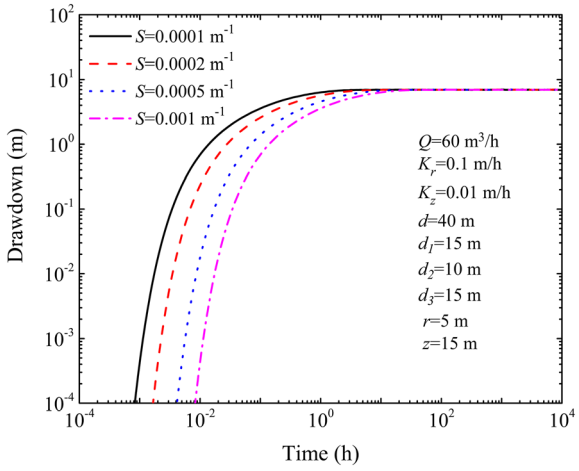

Figure 7. The effect of the aquifer specific storage on drawdown (S) with time.

drawdowns at early times. Moreover, drawdowns approach a steady state (i.e., curves are horizontal and parallel) when $t > 1$ hr, which is different from the previous case (the radial hydraulic conductivity). It is worth noting that the effect of further decreasing the length of the sealed section from 8 to 6 m on drawdown becomes negligible. Differences between drawdowns are larger for larger lengths of the sealed section (e.g., from 10 to 14 m) than for smaller lengths of the sealed section.

The effect of the ratio κ of the lengths of the pumping and injection sections ($\kappa = d_1/d_3$, for $d_1 \neq d_3$ and constant d and d_2) is shown in Figure 6b. As shown in Figure 6b, larger κ ratios result in smaller drawdowns. Drawdowns converge asymptotically toward a steady state for all scenarios. In addition, it is worth noting that changes in drawdown for smaller κ are larger than those for larger κ (from 1.0 to 1.8).

3.5. Aquifer Specific Storage

Figure 7 demonstrates how drawdown changes with time for different values of the aquifer specific storage (S = 0.0001, 0.0002, 0.0005, and 0.001 m^{-1}) and for the same other conditions as before, that is, $Q = 60$ m^3/hr, $K_r = 0.1$ m/hr, $K_z = 0.01$ m/hr, $d = 40$ m, $d_1 = 15$ m, $d_2 = 10$ m, and $d_3 = 15$ m, at $r = 5$ m and $z = 15$ m. It can be observed that drawdown decreases with an increase in the specific storage (S) at early times. In contrast, all drawdown curves for different values of the specific storage converge asymptotically to the same value at late times. When other conditions remain the same, an aquifer with large specific storage releases more water than an aquifer with small specific storage. Therefore, as shown in Figure 7, drawdown decreases with the specific storage at early times. Since the process of water release from the aquifer storage is almost complete at late times, all drawdown curves eventually approach the same asymptotic value after about 10 hr of operation and remain stabilized at late times. As a result, the impact of the specific storage on drawdown is insignificant at late times.

3.6. Pumping Time

It is also interesting to analyze how drawdown varies with distance for different pumping times ($t = 0.1$, 1, and 10 hr, and steady state). The other parameters in this scenario are again the same as before; that is, $Q = 60$ m^3/hr, $K_r = 0.1$ m/hr, $K_z = 0.01$ m/hr, $S = 0.0001$ m^{-1}, $d = 40$ m, $d_1 = 15$ m, $d_2 = 10$ m, and $d_3 = 15$ m at $r = 5$ m and $z = 15$ m. The analytical solution Equation 10 for the steady-state drawdown (see section 2.4) is utilized as a reference in this section. Figure 8 shows that drawdown changes only slightly with time for relatively small distances from the well, indicating that groundwater flow quickly reaches a quasi-steady state in the area close to partially penetrating wells. Additionally, Figure 8 also shows that the curves for $t = 10$ hr and the steady state almost coincide, indicating that the entire flow field in the single-well circulation system reaches steady state relatively quickly.

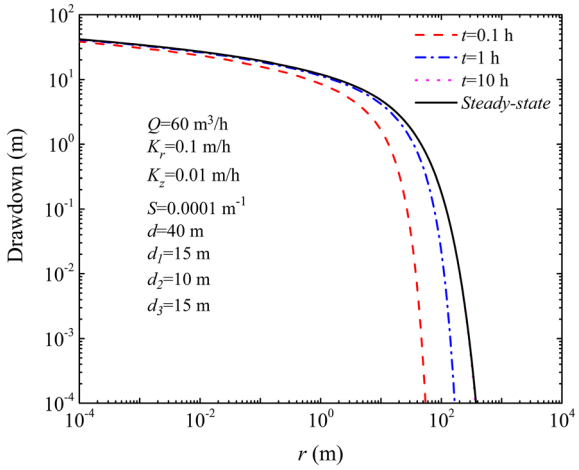

Figure 8. The effect of the pumping time (t) on drawdown with distance.

3.7. Sensitivity Analysis

To estimate the effects of various parameters on drawdown, the sensitivity analysis has been carried out for the specific storage S, the length of the sealed section d_2, and the radial and vertical hydraulic conductivities, K_r and K_z, respectively. Using the definition of the normalized parameter sensitivity proposed by Kabala (2001), one can obtain

$$Y_{m,n} = R_n \frac{\partial X_m}{\partial R_n}, \tag{11}$$

where $Y_{m,n}$ denotes the normalized sensitivity of the mth parameter R_n at the nth time and X_m is a function of R_n and n. A finite-difference equation proposed by Yeh (1986) (also used by Simunek & van

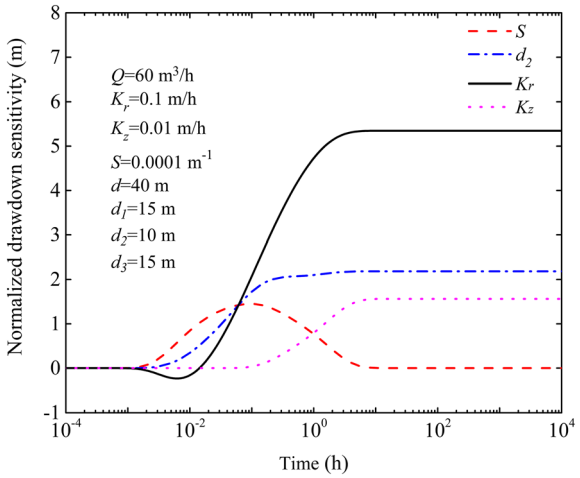

Figure 9. The sensitivity analysis of drawdown to selected parameters (the specific storage S, the length of the sealed section d_2, and the radial and vertical hydraulic conductivities, K_r and K_z, respectively).

Genuchten, 1996) can be used to approximate the partial derivative in Equation 11:

$$\frac{\partial X_m}{\partial R_n} = \frac{X_m(R_n + \Delta R_n) - X_m(R_n)}{\Delta R_n}. \quad (12)$$

The small increment ΔR_n of $0.01 \times R_n$ is used in this work, similarly as in Yeh (1986), Simunek and van Genuchten (1996), Huang and Yeh (2007), and Wen et al. (2013), with the latter two carrying out the sensitivity analysis of parameters for non-Darcian flow problems in a confined aquifer. Other parameters are as before: $Q = 60$ m^3/hr, $K_r = 0.1$ m/hr, $K_z = 0.01$ m/hr, $S = 0.0001$ m^{-1}, $d = 40$ m, $d_1 = 15$ m, $d_2 = 10$ m, and $d_3 = 15$ m, at $r = 5$ m and $z = 15$ m. Figure 8 shows the normalized sensitivities of drawdown with respect to the change of selected parameters. The sensitivity analysis indicates that these parameters do not have any impact on drawdown at early times and that each parameter has its own influence period on drawdown. It also indicates that drawdown is very sensitive to the change in the radial hydraulic conductivity. It is worth noting that the radial hydraulic conductivity K_r has a negative influence on drawdown in the period of 3×10^{-3} hr $< t < 2 \times 10^{-1}$ hr. The normalized sensitivity then starts increasing until about 4 hr when it stabilizes. The sensitivity of drawdown with respect to the lengths of the sealed section d_2 starts at about 3×10^{-3} hr, reaches the highest value at about 0.5 hr, and then remains stable. The sensitivity of drawdown associated with the specific storage S starts increasing at about 3×10^{-3} hr, reaches the peak value at about 0.1 hr, and then gradually decreases until about 15 hr. Finally, the influence of the vertical hydraulic conductivity on drawdown is small and negligible before 0.1 hr, then keeps increasing until about 10 hr, and then remains constant.

In practical engineering applications, the design of a single-well circulation groundwater heat pump needs to consider many factors, such as local hydrogeological conditions, thermal geological conditions, and the configuration of the well structure, in order to optimize the efficiency of the system and minimize its costs. As indicated by the sensitivity analysis in Figure 9, it is necessary to investigate hydrogeological conditions using pumping tests, in situ permeability tests, and geophysical surveys to obtain data related to hydraulic conductivities. The configuration of the well structure in real engineering applications then needs to be adjusted according to aquifer properties. As shown in Figure 6, shorter lengths of the sealed section result in larger drawdown, which indicates that the thermal breakthrough will occur sooner and the system will be less efficient. Although longer lengths of the sealed section could delay the thermal breakthrough, the cost of drilling the well and the electricity consumption for pumping and injection will increase. Therefore, factors such as the efficiency of the system, initial costs, and energy consumption should be comprehensively considered when designing a proper length of the sealed section for a single-well circulation groundwater heat pump system.

4. Conclusions

A general analytical mathematical model was developed in this study to investigate the characteristics of groundwater flow in a single-well circulation system. The governing partial differential equation is solved simultaneously with initial and boundary conditions by applying the Laplace and Fourier cosine transforms. The analytical solution for transient drawdown in the Laplace domain is obtained and then inverted numerically using the Stehfest method. The steady-state solution for drawdown in the time domain for a single-well circulation system is also developed. Additionally, the effects of different parameters on drawdown are also analyzed. The main research conclusions can be drawn as follows:

1. The contours for steady-state drawdown are symmetric around the horizontal midline of the aquifer and vary tremendously with distance from the well axis (in the case of $d_1 = d_3$). The drawdown contours around the sealed section are dense, indicating that the hydraulic gradient in this area is relatively large.

2. The length of the sealed section d_2 has a significant influence on drawdown in the case of $d_1 = d_3$. In the case of $d_1 \neq d_3$ and a constant length of the sealed section d_2, larger ratios of κ ($\kappa = \frac{d_1}{d_3}$) result in smaller drawdowns, while changes in drawdown become insignificant for further increases in κ values.
3. The spatial distribution of drawdown in a single-well circulation system is sensitive to the radial hydraulic conductivity K_r and the length of the sealed section d_2. Each parameter has its own influence period on drawdown.
4. Drawdown is not sensitive to parameters S, d_2, K_r, and K_z at early times, while it is very sensitive to these parameters at late times, particularly to the radial hydraulic conductivity, K_r.

Appendix A: Derivation of the Analytical Solution of the Mathematical Model

The governing equation in the Laplace domain is obtained by using the Laplace transform with respect to time t:

$$\frac{\partial^2 \bar{s}(r,\ z,\ p)}{\partial r^2} + \frac{1}{r}\frac{\partial \bar{s}(r,\ z,\ p)}{\partial r} + \frac{K_z}{K_r}\frac{\partial^2 \bar{s}(r,\ z,\ p)}{\partial z^2} = \frac{S}{K_r} p\bar{s}(r,\ z,\ p), \tag{A1}$$

where $\bar{s}$ is the Laplace transform of drawdown and p is the Laplace transform variable. The Fourier cosine transform is then applied to the term in Equation A1 with the second-order partial derivative with respect to the z coordinate:

$$F_c\left[\frac{\partial^2 \bar{s}(r,\ z,\ p)}{\partial z^2}\right] = \int_0^d \frac{\partial^2 \bar{s}(r,\ z,\ p)}{\partial z^2}\cos\left(\frac{N\pi z}{d}\right)dz = -\frac{N^2\pi^2}{d^2}\bar{\bar{s}}(r,\ N,\ p). \tag{A2}$$

Equation A1 is then rewritten by substituting Equation A2 as follows:

$$\frac{d^2\bar{\bar{s}}(r,\ N,\ p)}{dr^2} + \frac{1}{r}\frac{d\bar{\bar{s}}(r,\ N,\ p)}{dr} + \frac{K_z}{K_r}\left(-\frac{N^2\pi^2}{d^2}\right)\bar{\bar{s}}(r,\ N,\ p) = \frac{Sp}{K_r}\bar{\bar{s}}(r,\ N,\ p), \tag{A3}$$

in which $\bar{\bar{s}}$ denotes the Fourier cosine transform of drawdown and N (N = 1,2,3,.....) is the Fourier transform variable. After simplifying Equation A3, one obtains

$$\frac{d^2\bar{\bar{s}}(r,\ \mathrm{N},\ p)}{dr^2} + \frac{1}{r}\frac{d\bar{\bar{s}}(r,\ N,\ p)}{dr} - \left(\frac{K_z}{K_r}\frac{N^2\pi^2}{d^2} + \frac{Sp}{K_r}\right)\bar{\bar{s}}(r,\ N,\ p) = 0. \tag{A4}$$

Equation A4 can be rewritten as follows by defining $\delta = \frac{K_z N^2\pi^2}{K_r\ d^2} + \frac{Sp}{K_r}$:

$$\frac{d^2\bar{\bar{s}}(r,\ N,\ p)}{dr^2} + \frac{1}{r}\frac{d\bar{\bar{s}}(r,\ N,\ p)}{dr} - \delta\bar{\bar{s}}(r,\ N,\ p) = 0. \tag{A5}$$

Equation A5 is a linear second-order differential equation, which has the general solution as follows:

$$\bar{\bar{s}}(r,\ N,\ p) = C_1 I_0\left(\sqrt{\delta}r\right) + C_2 K_0\left(\sqrt{\delta}r\right), \tag{A6}$$

where C_1 and C_2 are integration constants, which can be determined using boundary conditions, and $I_0(x)$ and $K_0(x)$ denote the first and second kind modified Bessel functions of zeroth order with an argument x, respectively.

Applying the Laplace transform to Equations 3–5, the boundary conditions in the Laplace domain can be given as follows, respectively:

$$\frac{\partial \bar{s}(r,\ 0,\ p)}{\partial z} = 0, \tag{A7}$$

$$\bar{s}(\infty,\ z,\ p) = 0, \tag{A8}$$

$$\frac{\partial \bar{s}(r,\, D,\, p)}{\partial z} = 0. \tag{A9}$$

Using the Fourier cosine transform to the z coordinate in Equations A7–A9, we can obtain

$$\bar{\bar{s}}(\infty,\, N,\, p) = 0. \tag{A10}$$

Taking into account the property of modified Bessel functions of the first kind, substituting Equation A10 into Equation A6, and having $C_1 = 0$, Equation A6 then can be rewritten as

$$\bar{\bar{s}}(r,\, N,\, p) = C_2 K_0\left(\sqrt{\delta} r\right). \tag{A11}$$

Applying the Laplace and Fourier cosine transforms to Equation 6, one can obtain, respectively,

$$\lim_{r\to 0} r\frac{\partial \bar{s}(r,\, z,\, p)}{\partial r} = \begin{cases} \dfrac{-Q}{2\pi K_r d_1 p}\dfrac{1}{} & (0 \le z \le d_1) \\ 0 & (d_1 \le z \le d_1 + d_2) \\ \dfrac{Q}{2\pi K_r d_3 p}\dfrac{1}{} & (d_1 + d_2 \le z \le d) \end{cases} \tag{A12}$$

and

$$\lim_{r\to 0} r\frac{d\bar{\bar{s}}(r.N,\, p)}{dr} = \frac{-dQ}{2NpK_r d_1 \pi^2}\sin\left(\frac{N\pi d_1}{d}\right) - \frac{dQ}{2NpK_r d_3 \pi^2}\left[\sin\left(\frac{N\pi(d_1 + d_2)}{d}\right)\right]. \tag{A13}$$

From Equations A11 and A13, we can obtain the integration constant C_2:

$$C_2 = \frac{dQ}{2NpK_r\pi^2}\left[\frac{\sin\left(\dfrac{N\pi d_1}{d}\right)}{d_1} + \frac{\left[\sin\left(\dfrac{N\pi(d_1 + d_2)}{d}\right)\right]}{d_3}\right]. \tag{A14}$$

Substituting Equation A14 into Equation A11, we get

$$\bar{\bar{s}}(r,\, N,\, p) = \frac{dQ}{2NpK_r\pi^2}\left[\frac{\sin\left(\dfrac{N\pi d_1}{d}\right)}{d_1} + \frac{\left[\sin\left(\dfrac{N\pi(d_1 + d_2)}{d}\right)\right]}{d_3}\right] K_0\left(\sqrt{\delta} r\right). \tag{A15}$$

When $N = 0$, the term $\dfrac{K_z}{K_r}\dfrac{N^2\pi^2}{d^2} + \dfrac{Sp}{K_r}$ in Equation A4 becomes $\dfrac{Sp}{K_r}$. Here, we define $\omega = \dfrac{Sp}{K_r}$. Thus, the governing equation for this case can be written as

$$\frac{d^2\bar{\bar{s}}(r,\ 0,\ p)}{dr^2} + \frac{1}{r}\frac{d\bar{\bar{s}}(r,\, 0,\, p)}{dr} - \omega\bar{\bar{s}}(r,\, 0,\, p) = 0. \tag{A16}$$

A similar approach is applied to solve Equation A16 and boundary conditions. Finally, the general solution can be obtained as follows:

$$\bar{\bar{s}}(r,\, 0,\, p) = C_2{}' K_0\left(\sqrt{\omega} r\right). \tag{A17}$$

Applying the Fourier cosine transform to Equation A12, one has

$$\lim_{r\to 0} r\frac{d\bar{\bar{s}}(r,\, 0,\, p)}{dr} = \int_0^{d_1}\frac{-Q}{2\pi K_r d_1}\frac{1}{p}\cos\left(\frac{N\pi z}{d}\right)dz\Big|_{N=0} + \int_{d_1+d_2}^{d}\frac{Q}{2\pi K_r d_3}\frac{1}{p}\cos\left(\frac{N\pi z}{d}\right)dz\Big|_{N=0} = 0. \tag{A18}$$

Based on Equation A17, one can obtain

$$\lim_{r\to 0} r\frac{d\bar{\bar{s}}(r,\,0,\,p)}{dr} = -\lim_{r\to 0}\left[C_2{}'\sqrt{\omega}rK_1\left(\sqrt{\omega}r\right)\right] = -C_2{}'. \tag{A19}$$

Then, combining Equations A18 and A19, the integration constant C_2' in the case of $N=0$ can be obtained as

$$C_2{}' = 0. \tag{A20}$$

Then, substituting Equation A20 to Equation A17, one has

$$\bar{\bar{s}}(r,\,0,\,p) = 0. \tag{A21}$$

Using the inverse Fourier cosine transform to Equation A15, one can obtain

$$\bar{s}(r,\,z,\,p) = \frac{1}{d}\bar{\bar{s}}(r,\,0,\,p) + \frac{2}{d}\sum_{N=1}^{\infty}\bar{\bar{s}}(r,\,N,\,p)\cos\left(\frac{N\pi z}{d}\right). \tag{A22}$$

Finally, by substituting Equations A15 and A21 to Equation A22, we can obtain an analytical solution in the Laplace domain.

Appendix B: Derivation of the Steady-State Solution

Applying the Fourier cosine transform to the term of the second-order partial derivative of the z coordinate in Equation 9, one can obtain

$$F_c\left[\frac{\partial^2 s(r,\,z)}{\partial z^2}\right] = \int_0^d \frac{\partial^2 s(r,\,z)}{\partial z^2}\cos\left(\frac{N\pi z}{d}\right)dz = -\frac{N^2\pi^2}{d^2}\hat{s}(r,\,N). \tag{B1}$$

Substituting Equation B1 to Equation 9, one gets

$$\frac{d^2\hat{s}(r,\;\;N)}{dr^2} + \frac{1}{r}\frac{d\hat{s}(r,\,N)}{dr} + \frac{K_z}{K_r}\left(-\frac{N^2\pi^2}{d^2}\right)\hat{s}(r,\,N) = 0. \tag{B2}$$

By defining $\delta' = \frac{K_z}{K_r}\frac{N^2\pi^2}{d^2}$, Equation B2 can be simplified as follows:

$$\frac{d^2\hat{s}(r,\;\;N)}{dr^2} + \frac{1}{r}\frac{d\hat{s}(r,\,N)}{dr} - \delta'\hat{s}(r,\,N) = 0. \tag{B3}$$

The general solution of Equation B3 can be given as follows:

$$\hat{s}(r,\,N) = C_3 I_0\left(\sqrt{\delta'}r\right) + C_4 K_0\left(\sqrt{\delta'}r\right), \tag{B4}$$

where C_3 and C_4 are integration constants. Using the boundary condition of Equation 3 and considering the property of the first kind of modified Bessel functions, one can have $C_3 = 0$, then Equation B4 becomes

$$\hat{s}(r,\,N) = C_4 K_0\left(\sqrt{\delta'}r\right). \tag{B5}$$

Applying the Fourier cosine transform to Equation 6, one gets

$$\lim_{r\to 0} r\frac{d\hat{s}(r,\,N)}{dr} = \frac{-dQ}{2NK_r d_1\pi^2}\sin\left(\frac{N\pi d_1}{d}\right) - \frac{dQ}{2NK_r d_3\pi^2}\left[\sin\left(\frac{N\pi(d_1+d_2)}{d}\right)\right]. \tag{B6}$$

By integrating Equations B5 and B6, the constant C_4 can be obtained:

$$C_4 = \frac{dQ}{2NK_r\pi^2}\left[\frac{\sin\left(\frac{N\pi d_1}{d}\right)}{d_1} + \frac{\left[\sin\left(\frac{N\pi(d_1+d_2)}{d}\right)\right]}{d_3}\right]. \quad \text{(B7)}$$

Substituting Equation B7 into Equation B5, one gets

$$\hat{s}(r, N) = \frac{dQ}{2NK_r\pi^2}\left[\frac{\sin\left(\frac{N\pi d_1}{d}\right)}{d_1} + \frac{\left[\sin\left(\frac{N\pi(d_1+d_2)}{d}\right)\right]}{d_3}\right] K_0\left(\sqrt{\delta' r}\right). \quad \text{(B8)}$$

Using the inverse Fourier cosine transform to Equation B8, one can obtain

$$s(r, z) = \frac{1}{d}\hat{s}(r, 0) + \frac{2}{d}\sum_{N=1}^{\infty}\hat{s}(r, N)\cos\left(\frac{N\pi z}{d}\right). \quad \text{(B9)}$$

Finally, substituting Equation B8 to Equation B9, an analytical solution for steady-state conditions can be obtained (Equation 10).

Data Availability Statement

There are no data-sharing issues because any data used in this manuscript have been provided. Computer codes used in this manuscript are available upon request from the corresponding author.

Acknowledgments
The authors gratefully acknowledge the financial support from the Key Program of the National Natural Science Foundation of China (Grant 41430318), the National Scientific and Technical Support Program of China (Grant 2016YFC0801801), the National Natural Science Foundation of China (Grants 41572222, 41602262, and 41702261), and the China Scholarship Council (CSC 201806430053).

References

Abu-Nada, E., Akash, B., Al-Hinti, I., Al-Sarkhi, A., Nijmeh, S., Ibrahim, A., & Shishan, A. (2008). Modeling of a geothermal standing column well. *International Journal of Energy Research*, *32*(4), 306–317.
Ataie-Ashtiani, B., Shafei, B., Rashidian-Dezfouli, H., & Mohamadzadeh, M. (2012). Capture zone of a partially penetrating well with skin effects in confined aquifers. *Transport in Porous Media*, *92*(2), 437–457.
Banks, D. (2009). Thermogeological assessment of open-loop well-doublet schemes: A review and synthesis of analytical approaches. *Hydrogeology Journal*, *17*(5), 1149–1155.
Barua, G., & Bora, S. N. (2010). Hydraulics of a partially penetrating well with skin zone in a confined aquifer. *Advances in Water Resources*, *33*(12), 1575–1587.
Chang, C. C., & Chen, C. S. (2002). An integral transform approach for a mixed boundary problem involving a flowing partially penetrating well with infinitesimal well skin. *Water Resources Research*, *38*(6), 1071. https://doi.org/10.1029/2001WR001091
Chang, Y. C., & Yeh, H. D. (2009). New solutions to the constant-head test performed at a partially penetrating well. *Journal of Hydrology*, *369*(1), 90–97.
Chen, C. S. (1984). A reinvestigation of the analytical solution for drawdown distributions in a finite confined aquifer. *Water Resources Research*, *20*(10), 1466–1468.
Chen, S. J., Wu, L. C., & Liu, C. W. (2010). Analysis of contaminant transport toward a partially penetrating extraction well in an anisotropic aquifer. *Hydrological Processes*, *24*(15), 2125–2136.
Chiu, P. Y., Yeh, H. D., & Yang, S. Y. (2007). A new solution for a partially penetrating constant-rate pumping well with a finite-thickness skin. *International Journal for Numerical and Analytical Methods in Geomechanics*, *31*(15), 1659–1674.
Crump, K. S. (1976). Numerical inversion of Laplace transforms using a Fourier-series approximation. *Journal of the ACM (JACM)*, *23*(1), 89–96.
De Hoog, F. R., Knight, J. H., & Stokes, A. N. (1982). An improved method for numerical inversion of Laplace transforms. *SIAM Journal on Scientific and Statistical Computing*, *3*(3), 357–366.
Deng, Z., Rees, S. J., & Spitler, J. D. (2005). A model for annual simulation of standing column well ground heat exchangers. *Hvac&R Research*, *11*(4), 637–655.
Feng, Q., & Wen, Z. (2016). Non-Darcian flow to a partially penetrating well in a confined aquifer with a finite-thickness skin. *Hydrogeology Journal*, *24*(5), 1287–1296.
Galgaro, A., & Cultrera, M. (2013). Thermal short circuit on groundwater heat pump. *Applied Thermal Engineering*, *57*(1–2), 107–115.
Hantush, M. S. (1957). Nonsteady flow to a well partially penetrating an infinite leaky aquifer. *Proc. Iraqi Sci. Soc.*, *1*(10), 10–19.
Hantush, M. S. (1961). Drawdown around a partially penetrating well. *Journal of the Hydraulics Division*, *87*(4), 83–98.
Huang, Y. C., & Yeh, H. D. (2007). The use of sensitivity analysis in on-line aquifer parameter estimation. *Journal of Hydrology*, *335*(3–4), 406–418.
Kabala, Z. J. (2001). Sensitivity analysis of a pumping test on a well with wellbore storage and skin. *Advances in Water Resources*, *24*(5), 483–504.
Lin, Y. C., Yang, S. Y., Fen, C. S., & Yeh, H. D. (2016). A general analytical model for pumping tests in radial finite two-zone confined aquifers with Robin-type outer boundary. *Journal of Hydrology*, *540*, 1162–1175.
Luther, K., & Haitjema, H. M. (1999). An analytic element solution to unconfined flow near partially penetrating wells. *Journal of Hydrology*, *226*(3–4), 197–203.

Ni, L., Li, H. R., Jiang, Y. Q., Yao, Y., & Ma, Z. L. (2011). A model of groundwater seepage and heat transfer for single-well ground source heat pump systems. *Applied Thermal Engineering*, *31*(14–15), 2622–2630.
Novakowski, K. S. (1989). A composite analytical model for analysis of pumping tests affected by well bore storage and finite thickness skin. *Water Resources Research*, *25*(9), 1937–1946.
Papadopulos, I. S., & Cooper, H. H. Jr. (1967). Drawdown in a well of large diameter. *Water Resources Research*, *3*(1), 241–244.
Rybach, L. (2015). Innovative energy-related use of shallow and deep groundwaters—Examples from China and Switzerland. *Central European Geology*, *58*(1–2), 100–113.
Simunek, J., & van Genuchten, M. T. (1996). Estimating unsaturated soil hydraulic properties from tension disc infiltrometer data by numerical inversion. *Water Resources Research*, *32*(9), 2683–2696.
Sorensen, S.N., & Reffstrup, J. (1992). Prediction of long-term operational conditions for single-well groundwater heat pump plants. *In: Proceedings of the 27th Intersociety Energy Conversion Engineering Conference*, vol. 4, 109–104, 114.
Stehfest, H. (1970a). Algorithm 368: Numerical inversion of Laplace transforms [D5]. *Communications of the ACM*, *13*(1), 47–49.
Stehfest, H. (1970b). Remark on algorithm 368: Numerical inversion of Laplace transforms [D5]. *Communications of the ACM*, *13*(10), 624–625.
Theis, C. V. (1935). The relation between the lowering of the piezometric surface and the rate and duration of discharge of a well using groundwater storage. *Eos, Transactions American Geophysical Union*, *16*(2), 519–524.
Tu, K., Wu, Q., & Sun, H. Z. (2019). A mathematical model and thermal performance analysis of single-well circulation (SWC) coupled ground source heat pump (GSHP) systems. *Applied Thermal Engineering*, *147*, 473–481.
Wang, C. T., Yeh, H. D., & Tsai, C. S. (2012). Transient drawdown solution for a constant pumping test in finite two-zone confined aquifers. *Hydrology and Earth System Sciences*, *16*(2), 441–449.
Wen, Z., Liu, K., & Chen, X. L. (2013). Approximate analytical solution for non-Darcian flow toward a partially penetrating well in a confined aquifer. *Journal of Hydrology*, *498*, 124–131.
Wen, Z., Huang, G. H, & Zhan, H. B. (2008). An analytical solution for non-Darcian flow in a confined aquifer using the power law function. *Advances in Water Resources*, *31* (1), 44–55.
Wu, Q., Tu, K., Sun, H. Z., & Chen, C. F. (2019). Investigation on the sustainability and efficiency of single-well circulation (SWC) groundwater heat pump systems. *Renewable Energy*, *130*, 656–666.
Wu, Q., Xu, S. H., Zhou, W. F., & LaMoreaux, J. (2015). Hydrogeology and design of groundwater heat pump systems. *Environmental Earth Sciences*, *73*(7), 3683–3695.
Xu, S. H., & Rybach, L. (2003). Utilization of shallow resources performance of direct use system in Beijng. *Geothermal Resource Council Transactions*, *27*, 115–118.
Xu, S. H., & Rybach, L. (2005). Development and application of a new, powerful groundwater heat pump system for space heating and cooling. *In Proceedings World Geothermal Congress*, pp. 1–5.
Yang, S. Y., & Yeh, H. D. (2005). Laplace-domain solutions for radial two-zone flow equations under the conditions of constant-head and partially penetrating well. *Journal of Hydraulic Engineering*, *131*(3), 209–216.
Yeh, H. D., Yang, S. Y., & Peng, H. Y. (2003). A new closed-form solution for a radial two-layer drawdown equation for groundwater under constant-flux pumping in a finite-radius well. *Advances in Water Resources*, *26*(7), 747–757.
Yeh, W. W. G. (1986). Review of parameter identification procedures in groundwater hydrology: The inverse problem. *Water Resources Research*, *22*(2), 95–108.
Zeng, Y. F., Zhou, W. F., & LaMoreaux, J. (2017). Single-well circulation systems for geothermal energy transfer. *Environmental Earth Sciences*, *76*(7), 296.
Zlotnik, V., Chen, X. H., & Sun, B. (1998). Semi analytical evaluation of three-dimensional velocity near a partially penetrating well in an unconfined aquifer. *Groundwater*, *36*(3), 514–519.